Large Scale Floating Photovoltaics on Lake Nasser for Effective Power Production and Reducing Water Losses

Maria Fernanda Marbello[1/2], Zeyad Yasser[2], Richard Meyer[2]

[1] Hochschule für Angewandte Wissenschaften Hamburg/Suntrace GmbH, Hamburg (Germany)

[2] Suntrace GmbH, Hamburg (Germany)

Abstract

Lake Nasser is one of the world's largest artificial lakes. It is an important driver of Egypt's economy, and it is the base for increasing agricultural land use in the country. However, being located in one of the most arid regions the reservoir is experiencing strong water losses due to evaporation. With growing population, water and power demand are further rising, and are becoming a major concern for the Egyptian people. Floating photovoltaic systems are a mitigation to strong water evaporation, while simultaneously effectively producing power. This concept study identifies a site in the northwestern part of Lake Nasser. In this calm part of the reservoir around 56 km^2 might be suitable for installing FPV systems. Although this would be a very huge FPV field it only would cover around 1% of the Lake's surface. Various state-of-the-art floating PV structures have been analyzed. The maximum achievable installed power is 10.2 GW_p and would lead to an annual power production of approximately 21 TWh. Due to directly hindering evaporation, where floaters are covering the surface, combined with the evaporation leverage effect by cooling also surrounding water the annual evaporation reduction is estimated to reach a maximum of approximately 0.177 km^3.

Keywords: Floating photovoltaic systems, cooling effect, evaporation reduction, FPV hydro power synergy

1. Introduction

According to (FAO, 2016) Egypt is expected to meet the threshold for absolute water scarcity by 2030. Egypt's dominant water source is the Nile River. Since the filling of the Grand Ethiopian Renaissance Dam in Ethiopia started the Nile is experiencing an estimated yearly shortage of 13.5 km^3. This shortage of water has been rising tensions between Egypt, Sudan and Ethiopia. In addition, similarly to other countries on the African continent, Egypt has been affected by climate change, facing severe droughts that have had direct repercussions on water availability.

In southern Egypt a significant amount of water is lost due to the high evaporation rates of the Aswan High Dam Reservoir (AHDR). The huge Egyptian partition of the AHDR is called Lake Nasser. It forms one of the world's largest artificial lakes with a surface area of around 5,250 km^2. El-Shazli *et al.*, 2018 estimated a long-term annual evaporation loss of 2,007 mm averaged over the entire reservoir. This results in annual evaporation losses of 10.5 km^3. Due to climate change with rising temperatures and predicted harsher droughts, the evaporation rate -which is already among the highest in the world- is expected to increase further. Hence, the evaporation of Lake Nasser is regarded as a serious problem.

A second concern is Egypt's population growth. Together with further industrialization, a strongly rising electricity and water demand is expected. To meet such increasing energy demand, the government's Integrated Sustainable Energy Strategy has set renewable energy targets of 42% by 2035.

A solution to address both major issues is the use of floating solar photovoltaic panels (FPV) on Lake Nasser. Egypt is characterized by having a high solar resource potential, with an average of Global Horizontal Irradiance of 6.3 kWh/m^2 per day or 2285 kWh/m^2 per year. Due to low latitude and absent of rainy periods this remains relatively constant through the year. This represents an excellent resource for solar photovoltaic. However, such resource remains untapped as the PV installed capacity until 2019 was only 2.4 GW. This is still a shallow fraction of what could be achieved (The World Bank Group, 2021).

The purpose of this study is to propose a suitable site that allows cost-effective installation of large-scale FPV installation on Lake Nasser, while simultaneously reducing evaporation losses. It analyses state-of-the-art FPV technologies while considering and comparing their specific features in order to predict the potential power

doi:10.18086/swc.2021.08.01 Available at http://proceedings.ises.org

production and respective water evaporation savings from a practical perspective.

2. Floating photovoltaic systems: Technology overview

Floating solar, or FPV is an emerging fast-growing technology that makes use water bodies to produce renewable energy. Projections show that the number of projects will increase at an average rate of 20% until 2025 (Haugwitz, 2020). Although most of the FPV projects are relatively small in size with a mode of 1.7 MW, FPV plants of up to 150 MW are already operating.

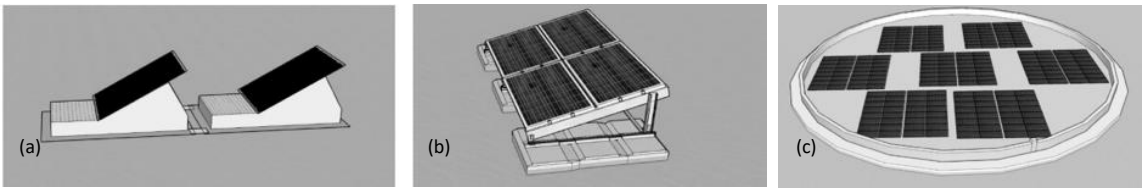

Fig. 1: Floating PV Structures - (a) Pure floats, (b) Modular rafts, (c) Membrane float (Source: DNVGL)

Among the many advantages of FPV systems are the opportunity to scale-up solar energy generation without competing for available land -a special asset for countries with high population density-, improvements of water quality owed to decreased algae growth, and of particular interest to this study, the reduction of water losses due to evaporation, and improved electricity generation of the PV modules as a result of lower operating module temperatures. The following sections cover the latter two more in detail. In addition to these, FPV systems can be strategically combined with hydropower plants to operate in synergy, where the solar array can take advantage of the already existing grid infrastructure, and together provide a more stable and flexible power generation.

FPV systems have a similar layout to the land-based ones, with the distinction that the modules and often the inverters are mounted on floating platforms. These floating structures are fixed with moorings either to nearby solid points on land or anchoring system on the water body's ground. Floating structures are typically divided into three main categories: pure floats, modular rafts, and membrane floats (see Fig. 1). Following are their main characteristics:

- Pure floats: These floating structures are characterized by the direct mounting of the PV modules onto solid floats that are typically made of High-Density Polyethylene (HDPE), making them robust to harsh conditions and strong wind speeds. They are designed to have a single, specific inclination angle, which depends on the float itself and the selected manufacturer. Typical values are between 5° and 22° (see Tab. 2).
- Modular rafts: These systems are distinguished by having a structural framework made of galvanized aluminum or stainless steel that is supported by floats. In this case, there is more flexibility regarding the tilt angle. Because the floaters do not fully cover the water surface where the system is placed, good ventilation under the modules allow for a cooling effect to be generated.
- Membrane floats: A relatively new technology where PV modules are attached to a reinforced membrane that is supported by a HDPE tubular ring. The whole structure formed by this ring and the membrane is providing buoyancy. Modules are placed plane on the membrane surface (tilt angle = 0°). The flat design is making this system more resilient to strong winds and waves.

The floating platform is an essential component of the PV installation, and the selected type will play a preponderant role in the project's priority: water evaporation reduction or energy generation.

3. Data and methods

3.1 Suitable site for large scale FPV on Lake Nasser

Selecting an adequate location for the FPV plant is key for a successful project. The selection criteria for the FPV system to be deployed on Lake Nasser is to find an area suitable for installing min. 4 GW_p, a location where investments costs are low, operation is safe, and preferably considering a region of Lake Nasser, which shows relatively high evaporation rates, so that potential water savings are maximized. According to (El-Shazli et al., 2018*)* which analyzes 3 evaporation measurement stations on Lake Nasser, highest evaporation of

2,884 mm is observed at the Raft station near the Aswan dam in the North. Reasons may be the slightly higher water temperatures in the North, but mainly the drying effect of the predominant NW to NE winds. Due to its quite large open water fetches in many parts of Lake Nasser significant wave height can build up, which would require installing substantially more expensive FPV or wave braking structures, which can withstand or destroy the waves. From planning other FPV projects we are aware of the high costs of mooring systems in deeper waters. Thus, although bathymetry was considered for site selection. Further, a nearby high voltage power line would be an advantage for lowering costs.

Considering all mentioned site selection criteria, a shallow, well protected part in the NW of the Lake is selected (see Fig. 2). Based on satellite-derived mapping of evaporation (Hassan, 2013; El-Shazli et al., 2018, p.) this part of the lake shows higher evaporation rates than the main lake – presumably due to higher water temperatures in this shallower part of the Lake Nasser. Hassan (2013) for this part indicates average annual evaporation of 2440 mm, while for the area of the Raft station only 2400 mm is given. For the Raft station this is substantially lower than the measurement derived. However, it must be noted that the evaporation rate at the selected site -and the one used on the present study- varies with respect to this figure. This is because the climatic conditions at the site under study are different, specifically temperature, relative humidity, wind speed and elevation. Further discussion is found in the following sections.

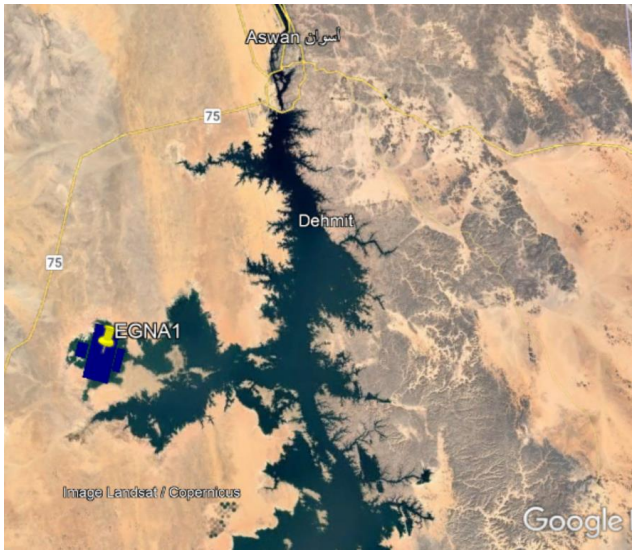

Fig. 2: Lake Nasser – Overview of selected site

The chosen remote part of the lake is well protected from larger waves building up occasionally in the main part of Lake Nasser. Distance from the 380 kV power line is only 10 km. Total area of this section of the lake is close to 90 km^2. Of this large site, several larger sub-areas have been identified which are in total providing suitable areas for FPV with a total of up to 56 km^2. The aim of this is to follow the Solar Energy Research Institute of Singapore (SERIS) recommendation of covering a maximum of 60% of a surface to prevent concerns about oxygen levels and amount of sunlight reaching the water.

3.2 Climatology of the site

The selected site was analyzed with regard to its solar resource potential using multiple data sources. An estimation of the expected long-term average Global Horizontal Irradiance (GHI) – called "best estimate" or P50 value – was performed, which is closely related to the potential photovoltaic power yields. Tab. 1 shows the main results. The inter-annual variability at this site is calculated using the long-term time series of PVGIS-SARAH and amount to 0.6 %, which is considered very low. Fig. 3 illustrated the annual cycle along with the average, maximum and minimum daily Global Horizontal Irradiation (GHI) and temperature to be expected.

Tab. 1: Climatic conditions of the selected site

Parameter	Value
Average air temperature	25°C
Maximum	35°C
Minimum	15°C
Max. relative humidity	55.4%
Min. humidity	4.6%
Max. wind speed	5.6 m/s
Min. wind speed	3.5 m/s
Direct Normal Irradiance	2759 kW/(m^2 a) = 315 W/m^2
Average of Global Horizontal Irradiance	2305 kW/(m^2 a) = 263 W/m^2

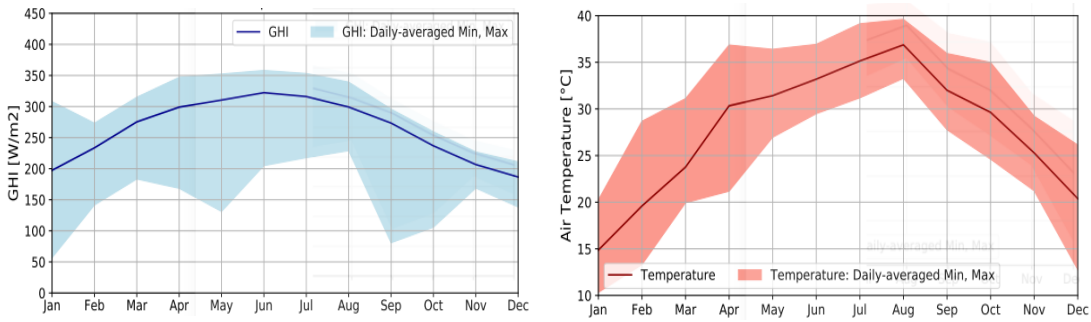

Fig. 3: Global Horizontal Irradiance (left) and Air Temperature (right) of the selected site. Lighter colours show maximum and minimum values of daily-averaged values during each month.

3.3 Engineering design

Conventional PV plant designs involve the utilization of the ideal inclination angle for the module, where the tilt angle is optimized taking into account the site's latitude in order to harvest the most irradiance that can hit the plane. However, for FPV plants this is a restricted parameter, as the tilt angle is limited by the design of the float. Other important parameters, such as the distance between rows and the necessary area for the platform are conditioned by the architecture of the floating system, and hence, by the manufacturer. For this reason, the potential of FPV in the selected site analyses the three currently available floating structures. Given that in the current market there are different manufacturers for each type of structure, nine designs from four different suppliers were studied. A summary of the designs and specifications considered on this study can be found on Tab. 2.

Tab. 2: FPV studied systems and their main respective design considerations

Supplier	Floating structure	Tilt angle and orientation	Pitch distance
A	Pure float	5°, south oriented	1.97 m
A	Pure float	12°, south oriented	1.97 m
A	Pure float	15°, south oriented	1.97 m
A	Pure float	22°, south oriented	1.97 m
B	Pure float	5°, south oriented	1.13 m
C	Modular raft	5° east-west oriented[1]	4.55 m
C	Modular raft	10° east-west oriented	4.55 m
C	Modular raft	15° east-west oriented	4.55 m
D	Membrane	0°	1.23 m

FPV plants are built in terms of blocks or islands, where their size will depend on the conditions of the site and characteristics of the project. A typical block size is 10 MWp. Hence, the present study has taken this value as the first premise for the design. A targeted DC/AC ratio of 1.2 has been established, and tier-1 modules and inverters have been considered.

There is no strict recommendation regarding the type of PV module for solar floating plants; however, dual-glass modules have shown more resilience against highly moisturized environments and together with their butyl sealant for the edges, electrical components can be hermetically protected (Kempe et al., 2017). Therefore, a bifacial 545 W_p module has been selected for the simulations. As for the inverters, the industry has not shown a clear preference regarding CAPEX, OPEX and yield for central and string inverters. Nevertheless, the general recommendation that for big plants, central inverters avoid the complex cabling and ohmic losses that string inverters would imply. Therefore, a central inverter has been used for the simulations.

3.4 Power generation: simulation parameters

The amount of electricity that a PV system can generate is site-dependent, being the quality of the solar

[1] East-west oriented systems are arranged in a way that half of the modules have an azimuth angle of -90° and the other half +90°

resource the main driver. Various factors play a role on the final energy outcome, and although the efficiency is related to the design and selected components, environmental factors need to be considered. The overall methodology to estimate the energy production for a FPV plant is similar as to a ground-mounted system. However, as the system lays above water, certain parameters will behave differently, namely the thermal parameters, soling, and mismatch. The following sub-sections discuss this further.

3.4.1 Thermal losses and cooling effect

One of the major advantages that is attributed to FPV systems is the so-called cooling effect, which enhances energy production compared to land-based systems. The temperature at which a solar cell operates is of significant importance, as it determines the performance of the module. It is a result of the incident solar radiation, ambient temperature, wind speed and wind direction (Dörenkämper et al., 2020). This is represented by the thermal loss factor, or U-value. The general rule is that lower ambient temperatures lead to lower operating cell temperatures, and hence to a better performance. The U-value is described by eq. (1):

$$U = U_0 + U_v \cdot w \qquad \text{eq. (1)}$$

Where U_0 is a constant component and the second term is a factor proportional to the wind speed, *w*. This equation represents the standard approach utilized on ground-mounted systems, where a value of 29 W/m^{2}K is utilized. However and as stated by (Lindholm et al., 2021), FPV systems have a different interaction with the environment, and its modelling will depend on the type of floating structure. The U-value should account for the heat loss on both surfaces of the module. Thus, eq.(1) can be rewritten as follows:

$$U_{total} = U_{front} + U_{back} \qquad \text{eq. (2)}$$

The reason behind it is that the heat transfer coefficient, which accounts for convection and thermal radiation that are necessary to calculate the temperature of the cell, is different when modules are cooled by air on both sides -as in the case of modular rafts and pure floats-, or when they are in thermal contact with water, and hence cooled by air on one side and water on the other. Lindholm et al., 2021 determine that floaters with direct thermal contact with water benefit the most and have U-values in the range of 78.7 - 94.2 W/m^{2}K, whereas floating systems that prevent the modules to have direct thermal contact with water have a similar behavior to land-based systems. On the other hand, structures that allow for ventilation are found to have a median U-value of 47 W/m^{2}K.

Even though high U-values have an influence on the energy yield, the relation between these two is not necessarily linear. Far after solar radiation, the temperature of the PV module has the greatest influence on the power output, but still, the extent to which such temperature is lowered depends enormously on the region. This was demonstrated by Dörenkämper et al. (2020), where two climatic zones were compared -a tropical and a temperate maritime climate- and results showed that although having relatively high U-values, the increase in yield compared to a reference land-based system was only of 3% and 6% respectively.

3.4.2 Adaption of meteorological data

Specific characteristics of a site of interest, such as relative humidity, pressure, wind speed and dry bulb temperature are collected on a Typical Meteorological Year (TMY) file, which is later used as input for the energy simulations. However, values do not always account for the conditions of FPV systems, especially wind speed (v_w) and ambient air temperature (T_a). For this reason, an adaption of these two elements has been done on the TMY file. Following *(Hsu, 1986)* approach, wind speed was corrected according to the following equation:

$$v_w = 1.17 v_{land} + 1.62 \frac{m}{s} \qquad \text{eq. (3)}$$

Where (v_{land}) refers to the wind speed above land. This approach has been taken for FPV stand-alone designs, such as the one done by (Umoette, 2016). Similarly, ambient air temperature, T_{air}, above water is lower than on land. In order to account for it, the following correction has been done:

$$T_a = 0.9282 T_{air} + 0.0246 T_w \qquad \text{eq. (4)}$$

Where T_w is the temperature underlying the water body. Eq. (4) is based on the model and findings from Charles Lawrence Kamuyu et al., 2018.

3.4.2 Soiling losses

Given that solar arrays operate under open sky, they are subject to the cumulation of dust, bird droppings, and depositions of microparticles that affect the system's performance. Such are known as soiling losses. Factors as dust mass concentration, wind speed, wind direction and relative humidity are major contributors (Javed, Guo and Figgis, 2017). Because representing the dynamic behavior that these variables have among each other is a very complex task, it is common to find simulations that utilize values in the range of 1-3% (World Bank Group, Solar Energy Research Institute of Singapore and Energy Sector Management Assistance Program, 2019). Such assumption is valid for ground-mounted systems, where typically the tilt angle is high enough to allow for self-cleaning, particularly during rainy seasons. However, such approach can underestimate the real effect of soiling on FPV systems as tilt angles are typically low.

Following the findings of (Kimber et al., 2006; Tamizhmani, Macia and Cano, 2014), soiling can be modeled as a linear degradation. Based on the results from Tamizhmani, Macia and Cano, 2014, an equation that describes the soiling loses as a function of the tilt angle has been determined:

$$y = -0.0002\beta^3 + 0.0112\beta^2 - 0.1732\beta + 2.0036 \qquad \text{(eq. 5)}$$

Where y is the percentage of soiling losses and β represents the module's tilt angle.

3.4.3 Mismatch losses

When the amount of irradiance that hit a string of modules is different, the so-called mismatch losses occur. In this case, the current of the panel with the lowest irradiance will drop, limiting the performance of the entire string. Ground-mounted systems usually adopt values of 1%. However, the constant motion of water together with waves, currents and wind make FPV systems subject of a constant movement, thus adding for this kind of losses. According to studies ran by (Dörenkämper et al., 2021) on sites with different wave categories and wave heights, the minimum value found for mismatch losses was 3%. On the same report, it was noted that flexible systems based on HDPE floaters were especially vulnerable to this effect. Hence, it can be assumed that the potential losses for pure-float systems is higher than 3%.

3.5 Evaporation reduction

Estimations for evaporation rates at Laker Nasser have been previously done by different authors. *El-Shazli* et al., *2018* elaborated a study comparing three different locations along the lake and used several methods to calculate daily evaporation values. However, this values cannot be directly assumed for the site under study of the present analysis, as evaporation strongly depends on the site's meteorological characteristics, and as it has been proven, small differences on air temperature, wind speed or relative humidity can lead to diverging results ELMekkawy, Salah and Abdel Wahab, 2018. For the present study, solar resource assessment was carried out which also provided the necessary input data to apply evaporation calculation using the Penman-Monteith Evaporation Model.

3.5.1 Penman-Monteith model

A number of empirical methos have been developed to estimate evaporation based on climatic parameters. The Penman-Monteith equation combines energy balance with mass transfer to estimate evaporation on open water bodies. This model is well known in the literature for its accuracy *(Van Zyl and De Jager, 1987)*, and therefore has been selected as the model for current evaporation estimation on the selected site. It is represented by eq.(6):

$$E = \frac{0.404\Delta(Q*-N)+\gamma\frac{900u_2(e_S-e_a)}{T+273}}{\Delta+\gamma(1+0.34u_2)} \qquad \text{(eq. 6)}$$

Where E is the evaporation rate, Δ the slope of saturation vapor pressure curve, Q* the net radiation in MJ/m^{2}d, N the soil heat flux density in MJ/m^{2}d, γ the psychometric constant, u_2 the velocity of the average wind at 2 m height, e_s the saturation vapor pressure in kPa and e_a the mean actual vapor pressure, also in kPa.

3.5.2 Water coverage ratio

A relevant factor influencing water evaporation is the amount of solar radiation that hits a surface. FPV reduces evaporation because it acts a barrier between such radiation and the water. This is known as direct evaporation. However, an indirect effect also occurs as a result of the cooled water in the surroundings of the FPV system, which indirectly prevents evaporation to occur. This study focuses solely on the direct evaporation.

Water Coverage Ratio (WCR) is defined as the percentage of the water surface that is in direct contact with a floater, and it will differ from floater type and supplier.

4. Results

4.1 Energy production

PVsyst software version 7.2.6 is applied for analyzing the performance for each floater manufacturer and for different configuration. A representative shading scene is built to assess the respective shading losses. All simulations are based on a site-specific typical meteorological year (TMY) with hourly time resolution as explained in section 3.2. Additionally, relevant loss factors resulting from the plant's location, components and configuration were assessed and considered for the simulation.

The simulations are based on blocks of 10 MW_p FPV. Fig. 4 shows the energy performance results of each floater type and for different configurations. The difference in the thermal parameters and the cooling effect, mismatch, panel orientation (landscape and portrait) and the number of modules that can be installed within the same area, plays a major role for the performance of each floater type.

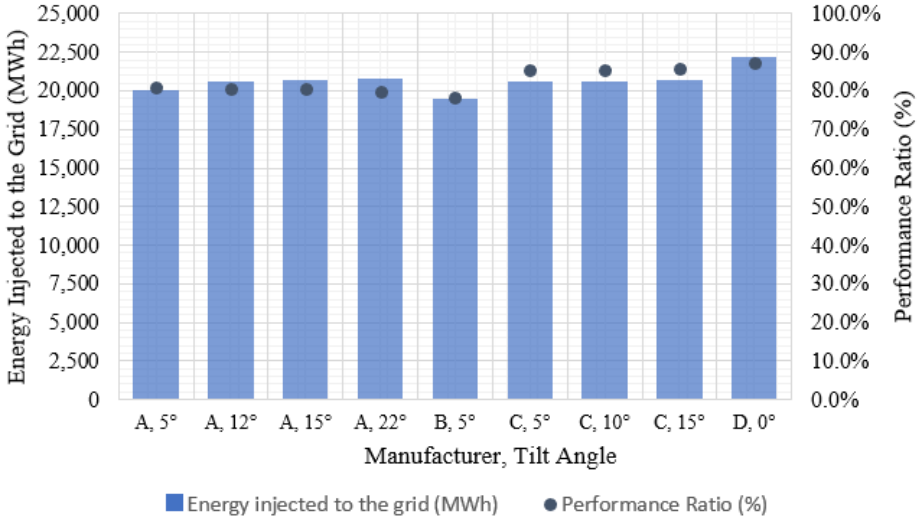

Fig. 4: Energy production and performance ratio for the analysed FPV designs

As it can be observed, all of the systems behave similar, where the difference between the highest and lowest generated energy is equivalent to 2,784 MWh. Taking a closer look to systems A and B, which belong to the same category -modular rafts- it is also observed that system A behaves better. This is the effect of lower distance between rows (pitch). System B, whose pitch distance is equal to 1.13 m, is being subject to higher shading losses, and hence, energy production is reduced.

Considering the effect of the tilt angle, the general trend is that the higher the tilt, the higher the energy production as systems can harvest most of the solar radiation hitting the module. However, this trend appears to be contradicted by systems A and C, particularly for those with angles of 10°, 12°, 15° and 22°. In the case of system C, such behavior results from the East-West orientation of the modules, which with an increasing angle, shading becomes more pronounced leading to less energy.

As it was previously discussed, the architecture and dimensions of the floating structure is not the same for every system; it varies from one manufacturer to the other. Hence, the required area for a10MWp block will differ among them, and as a result, the number of blocks that can be deployed on a restricted surface will be different. Taking this into consideration, an estimation of the number of blocks that fit the 56 km^2 of the selected site has been calculated. When a FPV system is deployed, blocks are not placed directly next to each

other as the water motion could cause them to hit against one another. For this reason, a distance of 15 m between blocks was included in the calculation. Based on this numbers, it is possible to scale up the energy potential for each system. Results are displayed on Tab. 3.

Tab. 3: Potential energy production per manufacturer based on their respective number of blocks

Manufacturer	$Area_{10MW\ Block}$ (km^2)	Nb. of blocks to fit the total are of the site	Electricity generation potential (TWh)	
			Min.	Max.
A	0.107	478	9.61	9.94
B	0.056	886	17.24	
C	0.048	1020	21.019	21.59
D	0.094	595	12.43	

4.2 Water savings from evaporation reduction

Water savings were calculated based on the evaporation rate obtained from the Penman-Monteith model, which resulted on an average of 9.23 mm/day. This value lays in the range of previous elaborated studies in the proximity of the region (El-Shazli *et al.*, 2018).

From Fig. 5 it can be observed that water savings differ significantly from one system to the other, reaching values of up to 177 Mio m^3 per annum. As discussed in section 3.5.2, this assessment is focused on direct evaporation, which is related to the WCR. Based on online available data and direct conversations with manufacturers, the WCR of each system has been estimated. Results of this, together with a summary of the area that each floating system would require to cover 10%, 50% and 100% of the site, as well as the installed capacity, energy production and water savings can be found in Tab. 4[1]. It is clear that the manufacturer whose floater covers entirely the surface where it is deployed is the one with the highest water savings. However, the highest energy production potential belongs to manufacturer C, which happens to have the lowest WCR. This is because as depicted in Tab. 3 the architecture of such system allows a larger number of blocks to be installed.

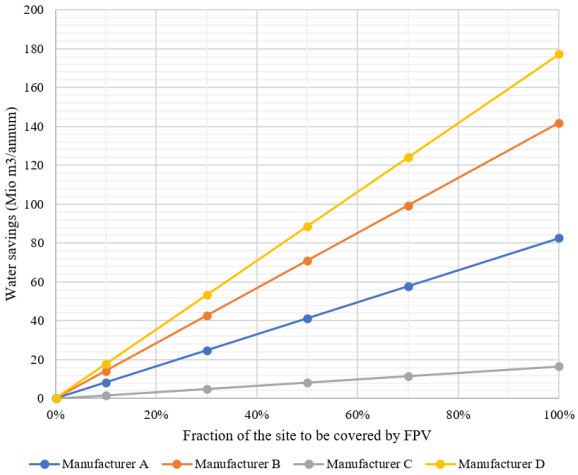

Fig. 5: Water savings as a function of the covered FPV area

Tab. 4: Area, installed capacity, energy production and water savings for each system considering different fractions of coverage area.

Manufacturer	WCR (%)	Covering 10% of the selected site				Covering 50% of the selected site				Covering 100%[2] of the selected site			
		A_{Block} (km^2)	IC (MW_p)	EP (TWh)	Water Savings (Mio. m3/annum)	A_{Block} (km^2)	IC (MW_p)	EP (TWh)	Water Savings (Mio m3/annum)	A_{Block} (km^2)	IC (MW)	EP (TWh)	Water Savings (Mio m3/annum)
A	48%	5.10	478	0.95	8.3	25.48	2,392	4.75	41.3	50.95	4784	9.59	82.6
B	85%	4.95	886	1.70	14.2	24.77	4431	8.54	70.9	49.51	8,863	17.07	141.8
C	10%	4.93	1,028	2.15	1.7	24.66	5,142	10.73	8.3	49.32	10,283	21.46	16.6
D	100%	5.26	596	1.20	17.7	26.31	2978	6.04	88.7	52,67	5,956	12.08	177.3

WCR: Water Coverage Ratio
A_{Block}: Area that the floating structure would occupy to cover the surface of the site's surface
IC: Installed capacity

[1] To illustrate conservative results, Energy potential (EP) is based on the lowest values of generated energy from each manufacturer
[2] 100% covered area = 56 km^2

5. Influence on hydropower electricity generation

An additional advantage of FPV systems is the possibility of deploying them on hydropower dams. Both systems have the potential of work in symbiosis, where the solar plant could operate during dry periods, and at the same time, hydropower could compensate for PV's intermittent power generation. However, even when both systems do not work in synergy, water saved from evaporation would mean additional water volume is available for electricity production. Following Gonzalez Sanchez *et al* 2021 rationale, the nominal power capacity of a hydropower station is described by eq. (7):

$$P = \eta \cdot \rho \cdot g \cdot Q \cdot h \qquad \text{eq. (7)}$$

Where η is the system's efficiency, ρ is the water density, g is acceleration of gravity, Q is the nominal water discharge of the turbines in m^3/s, and h is the hydraulic head in m. Given the volume of the water savings, $V\ (m^3)$, according to Gonzalez Sanchez *et al.*, 2021 a hydropower station could operate at full power for an additional number of hours, T, where

$$T = \frac{Q}{V} \qquad \text{eq. (8)}$$

Finally, the additional electricity is calculated by the product of $P \cdot T$.

According to the study realized by the Egyptian Electricity Holding Company and Hydro Plants Generation Company, 2016, the Aswan High Dam has a nominal capacity of 2,100 MW at a nominal water discharge Q of 11,043 m^3/s. In addition, the Aswan Low Dam with a nominal capacity of 592 MW also profits from the increased amount of water volume. Assuming FPV case D with the highest water savings of 177 km^3/annum, an additional 4.6 full load operation hours is given. This leads to an additional combined hydropower electricity production of 12 GWh per year. Compared to the very high additional electricity amount generated by this FPV layout this would be only 0.1% of this production. But compared to the current average hydro power generation of the Aswan High and Low Dam the reduction of evaporation on the upper reservoir provides a small but significant increase.

An additional advantage is the fact that FPV power production is highest during summer, when solar radiation is strongest and water levels of Lake Nasser decrease due to enhance evaporation. This is the time, when hydropower production is lowest in the annual cycle, but with more and more air conditioning installed power demand is strongly increasing.

The greatest advantage of connecting control of such huge FPV system with the Aswan High Dam hydropower system is, that the combination of the Aswan High and the Aswan Low Dam can be utilized as a huge battery system. Due to the direct connection between both large reservoirs continued water release from the lower dam can guarantee required minimum flow rates in the river downstream, while the turbines of the upper dam can be completely shut when FPV production is high. As the installed PV peak power of the proposed FPV cases utilizing the full 56 km^2 available depending on selected FPV technology is 4 to 10 times higher and solar irradiation at this site is very high at most days, there will be plenty of days where for around 10 h the water flow from the upper reservoir could be completely stopped. In addition, the saved water during the day leaves the opportunity to release more during evening and nighttime, when power consumption in Egypt also is raising. This excellent power storage utilization could be further improved when the turbines would be extended by pump functionality. For quantifying the full potential of such combination, it is recommended to analyze this in combined simulations.

6. Conclusions

Lake Nasser, Egypt's primary source of water and a major provider of hydroelectricity has the potential to deploy large-scale floating PV systems to produce electricity while simultaneously save water by reducing evaporation. The present study focused on a site located at the north-west of the lake, whose total surface area is equivalent to 90 km^2. However, to avoid environmental concerns related to water oxygenation and sunlight reaching the surface, a restricted area of 56 km^2 was selected to potentially deploy FPV systems.

After elaborating a solar resource assessment, findings showed that the solar characteristics at the site are excellent, with an average global horizontal irradiance equivalent to 263.1 W/m^2 or 2305 kW/(m^2 a). Four different types of floating structures belonging to state-of-the-art manufacturers are analyzed, while taking into consideration their design characteristics, such as allowed tilt angle and pitch. Additionally, the electrical behavior derived from environmental conditions of FPV systems were included, namely heat loss coefficient, soiling and mismatch losses. A modification of the Typical Meteorological Year (TMY) file -used to run simulations on the PVSyst software- was done in order to account for the environmental conditions that solar systems placed above water are subject of.

A 10MWp block design was used as a basis of the simulations. At the same time, it has been discussed that evaporation savings are a function of the area covered by the FPV system -the Water Coverage Ratio, which varies from manufacturer to manufacturer. Under these considerations, results showed that in spite of its differences, the four systems behave similarly producing values in the range of 19,265 MWh to 22,238 MWh. However, their dimensions play an important role in the total site's potential, as the required area to deploy a 10 MWp block varies significantly, allowing some systems to be deployed in greater number than others.

From a covered-area perspective, results showed that covering the total 56 km^2 with a modular raft floating system -the floater with the lowest WCR- there is a potential of generating 21.46 TWh. This results from the system's dimensions, which gives it the capacity of being deployed the most compared to the other three. On the other hand, water evaporation reduction reaches its peak levels with the membrane floating system is capable of saving up to 0.177 km^3 per year. This is due to its large WCR.

It must be noted that the evaporation figures presented on this report are the minimum amounts of water that could be saved, as the focus was on direct evaporation. If diffuse evaporation would be included, figures depicting water savings would be higher.

When placed on a hydropower plant, FPV systems offer the additional advantage of (1) working in synergy, strengthening the system's resilience against volatile climatic conditions, and (2) utilizing the saved water for extra electricity generation. In the case of Lake Nasser, an additional annual hydro power generation of 12 GWh could be expected for the case where around 1% of the Lake's surface are covered by the FPV technology, which is providing the highest water saving effect.

FPV is still an emerging technology, and the advantages that could be reached with this kind of systems is still to be untapped. Lake Nasser possesses many characteristics that make it ideal for the deployment of FPV, and many potential opportunities for the Egyptian country in terms of battling water scarcity and satisfying the electricity demand of its increasing population lay on the lake's water surface.

7. Acknowledgments

This work was supported by Suntrace GmbH. We would like to thank Simon Weber and Prof. Dr. Hans Schäfers for their contributions and support.

8. References

Charles Lawrence Kamuyu, W. *et al.* 2018. 'Prediction Model of Photovoltaic Module Temperature for Power Performance of Floating PVs', *Energies*, 11(2), p. 447. doi:10.3390/en11020447.

Dörenkämper, M. *et al.* 2020. 'The cooling effect of floating PV in two different climate zones: A comparison of field test data from the Netherands and Singapore'. doi:doi.org/10.1016/j.solener.2020.11.029.

Dörenkämper, M. *et al.* 2020. *Influence of Wave Induced Movements on the Performance of Floating PV Systems*. TNO-SE AC.

Egyptian Electricity Holding Company and Hydro Plants Generation Company. 2016. *Refurbishment of the generators of the Aswan High Dam*.

ELMekkawy, M.I., Salah, Z. and Abdel Wahab. 2018. 'Climatology of Lake Nasser in Egypt', 08(03), pp. 719–726.

El-Shazli, A. *et al.* 2018. 'Comparison of water balance method and alternative evaporation methods applied to the Aswan High Dam Reservoir', 149, pp. 117–131. doi:10.12854/erde-2018-349.

FAO, 2016. AQUASTAT Country profile - Egypt. Food and Agriculture Organization of the United Nations, Rome, Italy

Gonzalez Sanchez, R. *et al.* 2021. 'Assessment of floating solar photovoltaics potential in existing hydropower reservoirs in Africa'. doi:https://doi.org/10.1016/j.renene.2021.01.041.

Hassan, M. 2013. 'Evaporation estimation for Lake Nasser based on remote sensing technology', 4(4), pp. 593–604. doi:https://doi.org/10.1016/j.asej.2013.01.004.

Haugwitz, F. 2020. 'Floating solar PV gains global momentum', 22 September. Available at: https://www.pv-magazine.com/2020/09/22/floating-solar-pv-gains-global-momentum/.

Hsu, S.A. 1986. *Correction of Land-Based Wind Data for Offshore Applications: A Further Evaluation*. Available at: https://doi.org/10.1175/1520-0485(1986)016%3C0390:COLBWD%3E2.0.CO;2.

Javed, W., Guo, B. and Figgis, B. 2017. 'Modeling of photovoltaic soiling loss asa function of environmental variables', *Solar Energy*, 157, pp. 397–407. doi:10.1016/j.solener.2017.08.046.

Kempe, M.D. *et al.* 2017. 'Moisture ingress prediction in polyisobutylene-based edge seal with molecular sieve desiccant'. doi:https://doi.org/10.1002/pip.2947.

Kimber, A. *et al.* 2006. 'The Effect of Soiling on Large Grid-Connected Photovoltaic Systems in California and the Southwest Region of the Uniter States', *IEEE 4th World Conference on Photovoltaic Energy Conferenc*, pp. 2391–2395. doi:10.1109/WCPEC.2006.279690.

Lindholm, D. *et al.* 2021. 'Heat loss coefficients computed for floating PV modules'. doi:10.1002/pip.3451.

Tamizhmani, G., Macia, N.F. and Cano, J. 2014. 'Photovoltaic Modules: Effect of Tilt Angle on Soiling'. Arizona State University. Available at: DOI: 10.1109/PVSC.2014.6925610.

The World Bank Group. 2021. *Global Photovoltaic Power Potential - Egpyt.* Available at: https://globalsolaratlas.info/global-pv-potential-study.

Umoette, A. 2016. 'Design of Stand Alone Floating PV System for Ibeno Health Centre'. doi:http://dx.doi.org/10.11648/j.sjee.20160406.12.

Van Zyl, W.H. and De Jager, M. 1987. 'Accuracy of the Penman-Monteith Equation adjusted for atmospheric stability', 41(1–2), pp. 57–64. doi:https://doi.org/10.1016/0168-1923(87)90069-4.

World Bank Group, Solar Energy Research Institute of Singapore and Energy Sector Management Assistance Program. 2019. *Where Sun Meets Water: Floating Solar Handbook for Practitioners*. Washington D.C. Available at: https://openknowledge.worldbank.org/handle/10986/32804.